

Article

Corrosion Potential Modulation on Lead Anodes Using Water Oxidation Catalyst Coatings

Juliet F. Khosrowabadi Kotyk, Chi Chen  and Stafford W. Sheehan * 

Catalytic Innovations, Fall River, MA 02723, USA; juliet@catalytic-innovation.com (J.F.K.K.);
chi@catalytic-innovation.com (C.C.)

* Correspondence: staff@catalytic-innovation.com; Tel.: +1-347-927-4255

Received: 25 May 2018; Accepted: 4 July 2018; Published: 11 July 2018



Abstract: The oxidation of water to form oxygen gas provides charge balance for the cathodic deposition of metals, such as zinc, in the electrorefining industry. This is a corrosive, four-electron electrochemical reaction that causes deterioration of lead-silver alloy anodes employed in these processes. A sacrificial manganese oxide layer on the anode surface, formed in-situ from manganese sulfate, is used in industry to reduce the corrosion rate of these anodes by preferentially enabling water oxidation rather than lead dissolution. Still, it is poorly understood how the activity of manganese oxide as a water oxidation catalyst relates to its anticorrosive properties. Here, we show how the presence of water oxidation catalysts both formed in-situ (including the industry standard manganese oxide) and heterogenized prior to electrolysis on lead anodes affect the corrosion potential of these anodes. We find that corrosion potential under dynamic polarization conditions is the parameter most affected by the coatings formed in-situ and applied ex-situ prior to electrolysis.

Keywords: water oxidation; catalysis; electrochemistry; electrowinning; electrorefining; anode corrosion; electrocatalysis; cobalt oxide; manganese oxide

1. Introduction

Research on water oxidation catalysts to provide protons and electrons for solar fuel production is pursued around the globe, with thousands of studies published on the topic [1]. There has been comparatively little progress implementing this knowledge in practical and industrial systems, many of which still use catalysts developed several decades ago [2]. The gap between research investment and commercial use continues to widen as solar fuel integrated systems published today face challenges producing a positive economic return. Therefore, it is advantageous to first commercialize and de-risk the discrete components of a solar fuel integrated system (e.g., water oxidation catalysts, reduction catalysts, and photosensitive semiconductors [3]).

Water oxidation ($2\text{H}_2\text{O} \rightarrow \text{O}_2 + 4\text{H}^+ + 4\text{e}^-$, $E_{rev}^0 = 1.23$ V vs. RHE) is frequently cited as the half-reaction for fuel production, which is its purpose in nature. However, the electrochemical industry uses water oxidation and similar oxidative electrochemical half-reactions to produce metals, chlorine, and other feedstock independent of fuel. Reversible water oxidation and oxygen reduction are used in batteries, such as zinc-air batteries where reversible water oxidation catalysts improve energy efficiency [4]. Electrochemical coating processes, such as cathodic electrodeposition, where positively-charged metal ions are reduced on the surface of a substrate forming a conformal metal coating, use water oxidation to balance overall charges of the system [5].

Industrial electrorefining or electrowinning processes operate by similar principles. Lead alloy electrodes are widely used as anodes in industry and are assumed to have Faradaic efficiency near unity [2]. The lead anodes are electrically conductive, low cost and relatively stable at high potentials

and acidic conditions [6]. Corrosion of these anodes limits the lifetime of use, increases cost and can lead to contaminants in the products being produced in the electrorefining or electrowinning.

The efficiency of the water oxidation/oxygen evolution reaction (OER) determines the overpotential of the anode. This metric provides a means to assess the overall cell voltage, as high overpotential leads to increased cell voltage and reduced cell efficiency. Since high overpotential results in an increased cell voltage and, subsequently, a reduced cell efficiency, reducing overpotential under galvanostatic conditions (fixed anodic current density) has been proposed to promote the formation of denser surface oxide layers by controlling the consumption rate of Mn^{2+} ions at the surface to grow a thick and dense $\text{PbO}_2\text{-MnO}_2$ film [7]. A thicker protective layer reduces electrode Pb^{2+} dissolution, preventing corrosion.

In the commercial production of zinc by electrowinning, ZnO is dissolved in a sulfuric acid electrolyte, and pure Zn metal is cathodically deposited on aluminum metal cathodes. Lead-silver (PbAg) alloys are a common industrial anode for Zn electrolysis, as Ag is known to aid in protective lead dioxide (PbO_2) growth, lower overpotential, improve electrode conductivity, and reduce corrosion [8]. In zinc electrowinning, Mn^{2+} is additionally used to minimize lead anode corrosion. The Mn^{2+} deposits onto the electrode surface and acts as an inhibitor barrier between the electrolyte solution by forming a MnO_2 layer [9]. Formation of a dense, non-conductive MnO_2 film that adheres to the PbO_2 anode surface forms a dense mixed metal oxide layer. The oxide layer helps prevent dissolution of Pb^{2+} . Similar effects are seen from the inclusion of Co^{2+} ions in solution; however, evidence has been shown Co ions compete with silver in the anode for formation of active sites to catalyze water oxidation, while Mn^{2+} ions do not [10].

In this study, we explore the effect of Mn^{2+} and Co^{2+} separately in solution, which form catalytic metal oxide species in-situ, and a cobalt oxide-based heterogeneous water oxidation catalyst (as a model system, we use Co-dppe (cobalt 1,2-bis(diphenylphosphino)ethane)) [11,12], which is applied as an electrode coating ex-situ prior to electrolysis, on the electrode potential of PbAg anodes. This property, known as the open circuit potential (OCP), is the relative potential of the metallic working electrode to the reference electrode under equilibrium conditions, with net zero current across the electrode-electrolyte interface. Experimentally, we measure a quasi-OCP by determining the voltage where minimal current is supplied from the galvanostat. We use this as an approximation of the true electrode potential, since OCP is strictly defined as the equilibrium potential of the electrode in the absence of electrical connections. In corrosion chemistry, the OCP is also called the corrosion potential (E_{corr}). It is a thermodynamic parameter which indicates the tendency of the metallic electrode to freely corrode by participation in the electrochemical corrosion reactions with the surrounding medium. Generally, the more reactive the metal, the more negative its E_{corr} value, and the more thermodynamically unstable the electrode surface is.

Many studies analyze complex, expensive alloyed metal materials in Pb anodes. This study serves to deepen our understanding of the effect that practical additives have on the fundamental thermodynamic properties of industrially utilized PbAg anodes. Data gathered using these methods explore changes in equilibrium states of PbAg anodes under different catalytic additive conditions. Measuring the evolution of surface potential of these electrodes helps us to understand the long-lived intermediates for water oxidation, guiding us toward a more complete mechanistic understanding in the future.

2. Materials and Methods

Electrochemical experiments were performed in a 50 mL three-neck round bottom flask container using a standard three-electrode cell. A silver/silver chloride electrode (Ag/AgCl, Bioanalytical Systems, Inc., West Lafayette, IN, USA, $E = +198$ mV vs. RHE) and a Pt mesh wire were used as the reference and counter electrodes, respectively. The working electrode was a 3.5 cm² working area of an industrial PbAg alloy anode (1.0% w/w Ag, Republic Metals, Inc., Cleveland, OH, USA). Anodes were filed and

sanded prior to use to remove any native oxide layer or surface contaminants. All potentials reported were converted from vs. Ag/AgCl to vs. RHE using the following equation:

$$E_{RHE} = E_{Ag/AgCl} + 0.059(\text{pH}) + E_{Ag/AgCl}^0 \quad (1)$$

where $E_{Ag/AgCl}^0 = 0.1976 \text{ V}$ at $25 \text{ }^\circ\text{C}$ and $\text{pH} = -0.2$ for $1.6 \text{ M H}_2\text{SO}_4$. Thus, $E_{RHE} = E_{Ag/AgCl} + 0.059(-0.2) + 0.1976$, which can be simplified to $E_{RHE} = E_{Ag/AgCl} + 0.1858$.

The electrochemical experiments were performed using a Pine Wavedriver 10 or 20 potentiostat/galvanostat and Pine Aftermath software version 1.4.7881 (Durham, NC, USA). All of the electrochemical experiments were performed in $160 \text{ g}\cdot\text{L}^{-1}$ (1.6 M) H_2SO_4 (ACS grade, Fisher Scientific, Hampton, NH, USA) electrolyte. No substantial iR drop was observed under these electrolyte conditions and cell geometry.

The Mn^{2+} and Co^{2+} content was $5 \text{ g}\cdot\text{L}^{-1}$ (0.025 M). Metal ions were introduced into the electrolyte through the addition of $\text{Mn}(\text{NO}_3)_2\cdot\text{H}_2\text{O}$ and $\text{Co}(\text{NO}_3)_2\cdot\text{H}_2\text{O}$. Typical Mn^{2+} concentration in industrial zinc electrowinning electrolyte is in the range of $1\text{--}10 \text{ g}\cdot\text{L}^{-1}$, and $5 \text{ g}\cdot\text{L}^{-1}$ has been identified as an optimal concentration previously [9,10]. To drop-cast the heterogeneous water oxidation catalyst, a suspension of $50 \text{ mg}\cdot\text{mL}^{-1}$ Co-dppe in ethyl acetate was sonicated for 30 min. A 0.25 mL aliquot was drop-cast onto all sides of the electrode surface using a 1-mL syringe and a 25-G needle to apply 10 mg Co-dppe. Co-dppe was prepared using previously published methods [12].

The behavior of PbAg electrodes with different water oxidation catalysts present under anodic conditions was tested using standard electrochemical methods. Corrosion potential (E_{corr}) was determined using OCP measurements. Chronoamperometry (CA) and chronopotentiometry (CP) were measured for durations of 30 min, and cyclic voltammetry (CV) measurements were carried out at a scan rate of $5 \text{ mV}\cdot\text{s}^{-1}$.

Due to the high capacitance present in the PbAg electrodes from both charged Pb and Ag species, to obtain reproducible potentiodynamic polarization curves chronoamperograms were measured at different potentials with 120 s hold times. This procedure allowed adequate time for the electrode to discharge and equilibrate at the chosen potential. Using this approach, Tafel plots were generated by scanning from -2.180 to 2.020 V in 200 mV increments, with no relaxation period between steps. These data were compared to linear sweep voltammetry (LSV) measurements between 2.2 and -0.11 V , which were taken at a slow scan rate of $200 \text{ }\mu\text{V}\cdot\text{s}^{-1}$ to control for electrode capacitance in order to probe different states of electrode surface polarization.

3. Results

3.1. Pb Anodes

The electrochemical behavior of Pb, and the more commonly used PbAg, anodes is relatively well known. In general, a series of reactions occur at the electrode surface that occur depending on the applied potential [2,13,14]. The first reaction (Equation (2)) is the interaction of the Pb anode surface with the sulfate ions from the H_2SO_4 solution to form a semi-permeable PbSO_4 layer on the surface at potentials near -0.21 V vs. RHE in $1.6 \text{ M H}_2\text{SO}_4$ ($\text{pH} = -0.2$) [15]:



At higher applied potential (higher than $+1.14 \text{ V}$) we find the formation of a PbO_2 species from PbSO_4 (Equation (3)):



Oxygen evolution ($E = 1.23 \text{ V}$ vs. RHE + η) occurs further in this region since it satisfies the overpotential (η) required for PbO_2 to catalyze water oxidation. We measured the electrode potential (E_{corr}) of the pristine PbAg electrode to be -0.26 V , which corresponds to the equilibrium potential of

PbSO₄ formation [16]. CVs showed known redox features of the Pb component of the anode, as shown in Figure 1, including the Pb/PbSO₄ redox wave at −0.31 V vs. RHE and PbO/Pb at −0.24 V vs. RHE. Similar to other published reports on PbAg anodes [2], we observe the PbO₂/PbSO₄ redox wave at 1.59 V vs. RHE as well as the onset of the OER at 1.92 V vs. RHE.

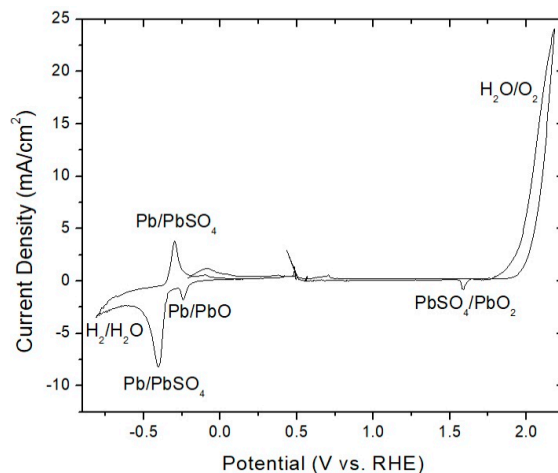


Figure 1. Cyclic voltammogram of a PbAg anode in 1.6 M H₂SO₄ with relevant redox features labeled, scan rate 5 mV·s^{−1}.

Potentiostatic CA with a 2.06 V applied potential over 30 min gave 17 mA·cm^{−2} current density and generated a substantial number of oxygen bubbles on the anode surface. An OCP measurement after polarization was 1.69 V indicating a highly polarized species, which is consistent with Ag₂O₂ produced at the surface of the electrode. The Ag₂O₂ is a mixed silver (I, III) oxide (Ag⁺Ag³⁺O₂) layer that increases OER activity and has been observed previously on PbAg anodes [8]. Galvanostatic CP at a constant applied current density of 50 mA·cm^{−2} over 30 min gave a higher potential of 2.19 V. This polarization also generates the same Ag₂O₂ surface species, indicated by the OCP performed afterwards resting at an equilibrium potential of 1.69 V.

Similar to prior studies on PbAg anodes, we found that the surface potential of the PbAg electrode and its activity toward oxygen evolution is dynamic and dependent on the stabilization of oxidized species on its surface. As shown in Figure 2, and consistent with the hypothesis from McGinnity and Nicol that this species is a high-potential silver oxide, its potential does not change as the surface properties of the PbAg anode are altered by either Mn²⁺/Co²⁺ in-situ or ex-situ Co-dppe water oxidation catalyst coatings. This common highly polarized species necessitates discharging the electrode surface to explore the lower-potential phenomena that are more closely related to the effect of catalytic additives. To accomplish discharging, potentiodynamic polarization via LSV experiment from 2.2 to −0.11 V was used, and the OCP reached during this voltammetric scan was found to be tunable based on the catalytic transition metal cation present in solution. In this study, we focus on Co²⁺ and Mn²⁺.

OCP performed directly after LSV was found to result in the same E_{corr} as found after leaving the electrode immersed in H₂SO₄ overnight, $E_{corr} = 0.01$ V, which is close to the extrapolated PbSO₄/PbO equilibrium potential [14].

There are four oxidative equilibrium states that we observed under open circuit conditions before and after electrolysis with high reproducibility and accessibility:

- Pre-electrolysis: The electrode surface upon immersion into 1.6 M H₂SO₄, prior to electrolysis. We observed that this state persists for days, with an E_{corr} on an unmodified PbAg surface of −0.25 V vs. RHE.

- Highly polarized: This state is accessed by measuring OCP immediately after sufficient electrode polarization for the formation of oxygen bubbles. It possesses a short lifetime (<1 h) and exhibits the same E_{corr} between trials independent of $\text{Co}^{2+}/\text{Mn}^{2+}/\text{Co-dppe}$ presence or concentration. These attributes suggest that it is indicative of a charged silver species, as proposed previously, with an E_{corr} of approximately 1.69 V vs. RHE.
- Polarized dynamic equilibrium: This equilibrium state is defined as the OCP having the lowest measured current reached during potentiodynamic polarization (0.14 V vs. RHE for unmodified PbAg; see Table S1 and Figure S1) immediately after electrolysis and varies dependent on the electrode surface coating ($\text{Co}^{2+}/\text{Mn}^{2+}/\text{Co-dppe}$).
- Resting equilibrium: This state corresponds to the second OCP reached during potentiodynamic polarization; the same value is also reached if the electrode is left sitting in the H_2SO_4 electrolyte for a day after electrolysis (0.01 V vs. RHE for unmodified PbAg). Similar to the polarized equilibrium potential, this OCP varies dependent on the electrode surface coating or formation of a dense mixed oxide layer.

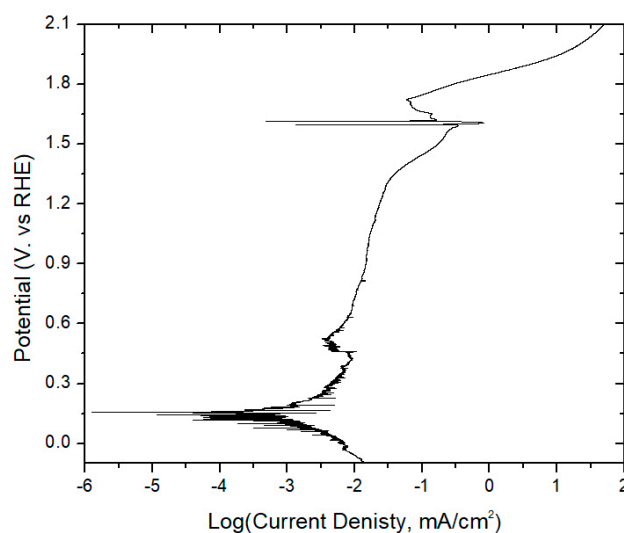
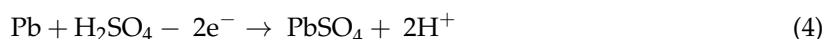


Figure 2. Example potentiodynamic polarization curve (scan rate: $50 \mu\text{V}\cdot\text{s}^{-1}$) of a PbAg anode in 1.6 M H_2SO_4 with open circuit features indicative of electrode surface polarization states, with the open circuit E_{corr} at the most negative Log (Current Density) being variable based on the catalyst present in solution ($\text{Mn}^{2+}/\text{Co}^{2+}$). The above data were gathered immediately after 30 min of electrolysis at 2.06 V vs. RHE.

While there are further reduced equilibrium states that can be accessed on these anodes, to remain relevant to industrial electrolysis conditions, we focus on oxidative equilibrium states [14]. Corrosion occurs at the surface of the electrode, which becomes predominantly PbSO_4 when immersed in H_2SO_4 . To estimate the pre-electrolysis potential when the electrode is submerged in electrolyte but has not been polarized we can use the following equations:



An initial film of PbSO_4 is formed upon contact and chemical reaction with the sulfuric acid. Dissociation of sulfuric acid occurs in two steps (Equations (5) and (6)) and solutions with acid

concentration higher than 0.5 M contain bisulfate (HSO_4^-) ions so that the overall reaction responsible for the formation of PbSO_4 is as follows [17]:



$$E_0 = -0.302 - 0.029\text{pH} - 0.029 \log(\text{HSO}_4^-) \quad (8)$$

Using Equation (8), the standard potential for the initial PbSO_4 film can be calculated as -0.30 V. The 40-mV difference between that value and the experimental OCP of -0.26 V may be explained by the presence of Ag metal. These anodes contain 1% Ag, which has a substantially higher reduction potential than Pb or PbSO_4 [18], which may shift the pre-electrolysis potential to be more positive.

3.2. In-Situ Coatings

With baseline electrochemical behavior of the PbAg anode established, we next studied the effect of Mn^{2+} and Co^{2+} solution-phase additives on the electrode potential. Evidence from prior studies suggests that these ions in solution become incorporated into a dense oxide layer on the electrode surface in situ, which helps to prevent Pb^{2+} ion dissolution and corrosion [19–21]. We thus expect the E_{corr} to become more positive with inclusion of these ions in solution.

Mn^{2+} is used as an inhibitor to protect these PbAg anodes from corrosion in the electro-winning industry. The E_{corr} of a PbAg electrode with a sulfuric acid electrolyte containing $5 \text{ g}\cdot\text{L}^{-1}$ Mn^{2+} is correspondingly -0.21 V vs. RHE, 43 mV more positive than without the Mn^{2+} in solution. On the other hand, the E_{corr} of a PbAg electrode with a sulfuric acid electrolyte containing $5 \text{ g}\cdot\text{L}^{-1}$ Co^{2+} is -0.24 V, which is only 20 mV more positive than the electrode without any solution-phase metal ion additives. All three of the pre-electrolysis E_{corr} values are close to one another, yet we know from both practical industrial use and studies published on corrosion in this system [2,6,7,13,22], that Mn^{2+} has an effect toward preventing anode corrosion.

This inhibitor effect is more pronounced in both the polarized equilibrium, taken during potentiodynamic polarization scans, and resting equilibrium taken both after polarization and after equilibration overnight. After polarization, the Mn^{2+} or Co^{2+} became incorporated into the anode as a component of the dense metal oxide surface, mixing with PbO_2 . This phenomenon is most evident in the E_{corr} values measured during potentiodynamic polarization (Table 1), where the presence of Co^{2+} increases anode surface potential by over 1.4 V and Mn^{2+} by over 0.8 V. By measuring the PbAg anodes in this manner, our aim is to probe the potential of the transient mixed oxide that forms on the Pb surface so that we can better understand the true E_{corr} of the active anti-corrosive species. That the polarized dynamic equilibrium surface potential changes based on the ion present in solution suggests that we are, indeed, measuring a film that is incorporating or otherwise significantly interacting with the catalytic metal cations. Thus, while care must be taken not to read too much into the data at high potentials where there are other processes occurring, these surface potentials that we measure under these conditions may be likened to the surface potential of MnO_x and CoO_x water oxidation catalysts [23–26].

Table 1. E_{corr} values (V vs. RHE) measured under open-circuit conditions during different equilibrium states of the PbAg electrode in 1.6 M H_2SO_4 . The “Polarized Equilibrium” state accessed by linear sweep voltammetry after electrolysis is highlighted in bold below as the most dependent on the catalytic metal ion present in solution.

Solution Additive	Pre-Electrolysis E_{corr} (V)	Highly Polarized E_{corr} (V)	Polarized Eq. E_{corr} (V)	Resting Eq. E_{corr} (V)
None	−0.26	1.69	0.14	0.01
$5 \text{ g}\cdot\text{L}^{-1}$ Co^{2+}	−0.24	1.69	1.60	0.04
$5 \text{ g}\cdot\text{L}^{-1}$ Mn^{2+}	−0.21	1.69	0.99	0.12

After further equilibration with the solution, the E_{corr} values decrease further as the native $PbSO_4$ surface is regenerated under resting equilibrium. These E_{corr} values suggest that the Mn^{2+} solution produces a more thermodynamically stable $PbSO_4$ -based surface than the Co^{2+} solution. The cause of this stabilization has been also ascribed to competitive adsorption between Co-based and Ag-based surface species, while the Mn-based species work synergistically with Ag [10].

CVs of each electrode show the redox features of the Pb component of the anode have all shifted to more cathodic values, suggesting that the Pb has now become easier to oxidize. With either catalytic metal cation present in the electrolyte, the Pb/ $PbSO_4$ quasi-reversible redox wave appears at approximately -0.46 V vs. RHE, which is 150 mV more cathodic than the case of the PbAg anode in H_2SO_4 without any catalytic metal additives. The Pb/ PbO feature is also cathodically shifted to -0.32 V vs. RHE and has substantially increased in magnitude, with its integrated area increasing by a factor of five (for Co^{2+}) to a factor of 10 (for Mn^{2+}), suggesting that more PbO is formed when the catalytic metal additives are used. One possible reason for this shift and current enhancement is further oxidation of Pb to PbO during the anodic sweep, catalyzed by the presence of Mn^{2+} or Co^{2+} in a dense mixed oxide surface layer along with PbO. A smaller, yet still noticeable cathodic shift and increase in magnitude in the $PbSO_4/PbO_2$ feature (1.57 V vs. RHE) may also be caused by the same phenomenon. In our continuing work, we plan to determine the oxidation states of Pb under these industrially-relevant conditions using in-situ X-ray photoelectron spectroscopy (XPS) to test this hypothesis.

From both the CVs in Figure 3 and the OER onset potentials in Table 2, it is clear to see that these CoO_x and MnO_x species act as water oxidation catalysts, as well as anticorrosion layers. By improving catalytic activity for water oxidation, the active catalytic mixed metal oxide passivates the PbAg anode surface and provides a driving force for hole transfer into water, preventing lead oxidation in the substrate anode from causing over-oxidation of the lead and dissolution. In this manner, these water oxidation catalysts build an in-situ anticorrosion layer that is rapidly removed from the anode due to the harshly acidic electrolyte conditions. From this point, we hypothesize that if a water oxidation catalyst can withstand the harsh conditions in zinc refining, it may bypass the need for a sacrificial in-situ catalyst in the electrolyte, thus reducing metal consumption in these processes. We investigate this pathway further in our experiments in Section 3.3, where we measure the effect of a heterogeneous water oxidation catalyst on the surface potential of the PbAg anode under similar conditions.

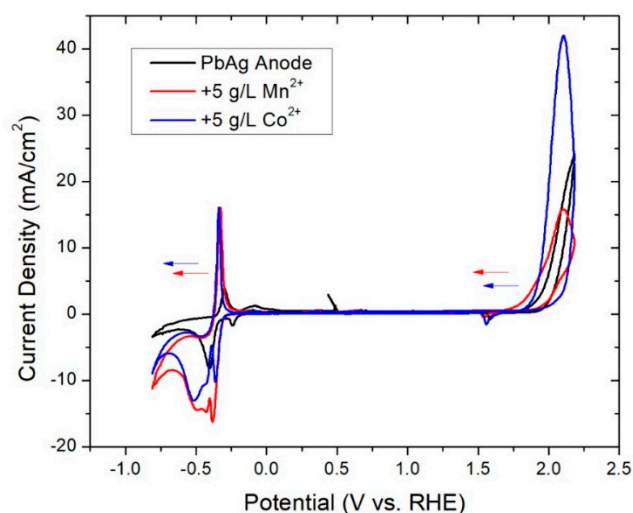


Figure 3. Cyclic voltammograms (scan rate $5\text{ mV}\cdot\text{s}^{-1}$) of the PbAg anode in $1.6\text{ M H}_2\text{SO}_4$ electrolyte, as seen in Figure 1, alongside identical samples that were subjected to the same electrolysis conditions with Co^{2+} (blue) or Mn^{2+} (red) ions in solution. Arrows indicate direction of redox feature shifts with additives present.

Table 2. Quantification of cathodic shifts in CV features as catalytic metal additives are included in solution. The Pb/PbSO₄ redox couple represents a quasi-reversible process, while the others reported below are irreversible.

Solution Additive	Pb/PbSO ₄ <i>E</i> _{1/2} (V)	Pb/PbO <i>E</i> _{Pb/PbO} (V)	PbSO ₄ /PbO ₂ <i>E</i> _{PbSO₄/PbO₂} (V)	OER Onset <i>E</i> _{OER} (V)
None	−0.31	−0.24	1.59	1.92
5 g·L ^{−1} Co ²⁺	−0.50	−0.36	1.56	1.89
5 g·L ^{−1} Mn ²⁺	−0.46	−0.32	1.57	1.82

The onset of OER with the Mn²⁺ cation in solution is at 1.82 V vs. RHE, which is 100 mV lower than the PbAg anode alone, and it has been shown that further increasing concentration of Mn(II) will lower the OER overpotential [6]. At high potentials, Mn²⁺ is oxidized to form stable MnO₂, which adheres to the PbO₂ layer and forms a dense mixed metal oxide [27]. CA at an applied potential of 2.06 V vs. RHE (>200 mV higher potential than the OER onset; see Figure 4) over 30 min resulted in over 90 mA·cm^{−2} current density. An OCP measurement after polarization initially gave the same highly polarized species that we see in all samples at 1.69 V vs. RHE, which the prior literature suggests to be Ag₂O₂ [7], as discussed previously.

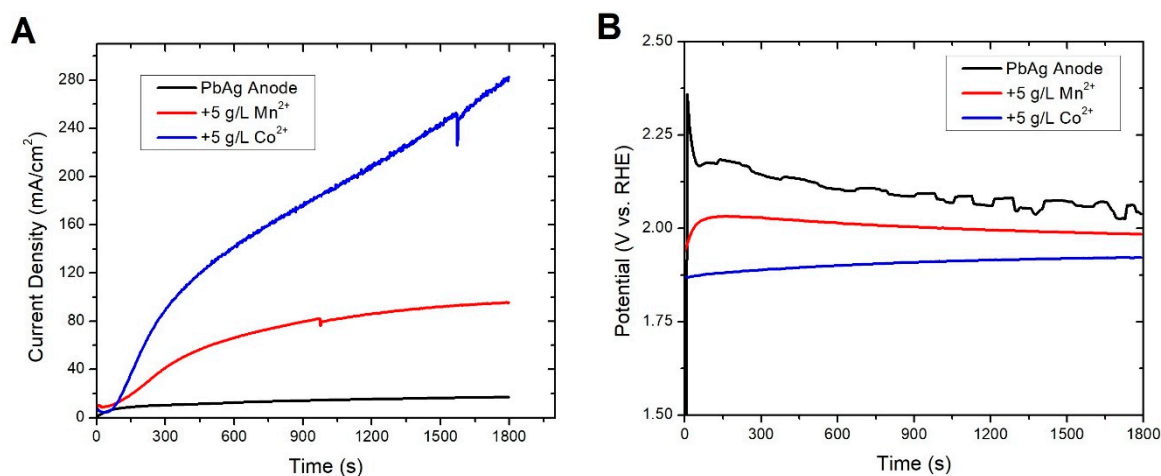


Figure 4. (A) Chronoamperograms at constant potential (2.06 V vs. RHE) and (B) chronopotentiograms under the three electrolyte conditions tested, with the Co-containing electrolyte in blue, Mn-containing electrolyte in red, and the PbAg anode without any water oxidation catalytic metal additives in black.

CP at an applied current density of 50 mA/cm² over 30 min required approximately 100 mV less potential than the PbAg electrode in unmodified electrolyte (1.89 V vs. RHE), similar to the effect seen when MnO₂ is alloyed into the electrode [23], providing further evidence that a lead-manganese mixed metal oxide is formed in-situ. If OCP is measured after either of the above CA or CP experiments, one will find a surface potential of 1.69 V across all electrolyte conditions due to the proposed Ag₂O₂ highly polarized surface species. To probe the surface features with lower potentials, LSV from 2.2 V to −0.11 V was used to reduce the charged surface species and access the catalytic metal-dependent species that we observe is in dynamic equilibrium with the electrolyte during polarization. The potential that we find of this species in the case of Mn²⁺ at the lowest Log (Current Density) value is 0.99 V vs. RHE, much more positive than the PbAg electrode. One explanation for this species may be that the electrode corrosion is inhibited by a MnO₄[−] species [9]. OCP measurements performed directly after the LSV scan or after leaving the electrode immersed in H₂SO₄ overnight gave a resting equilibrium value of 0.12 V, indicating that some of the charge of the mixed metal oxide on the surface is retained over longer timescales.

In particular, the OCP values measured during LSV immediately after electrolysis are found to be highly reproducible, and their magnitude suggests substantial modification of the surface properties of the electrode by the solution-phase catalytic metal additive. The effect on CA and CP measurements with Co^{2+} is even more pronounced, with over $280 \text{ mA}\cdot\text{cm}^{-2}$ current density after 30 min of electrolysis. CP at an applied current density of $50 \text{ mA}\cdot\text{cm}^{-2}$ over 30 min gave a drop in potential compared to the PbAg electrode (1.79 V) due to the conductive nature of Co^{2+} [21]. The same effect, where the OCP after electrolysis is pinned to 1.69 V, is seen with Co^{2+} , and LSV is used to reduce the charged surface species to find a Co^{2+} -dependent surface potential of 1.60 V vs. RHE, indicating a highly charged Co species compared to Mn^{2+} . The electrode charge drops further to a resting state of 0.04 V, however, which is a lower E_{corr} than the system that results from Mn^{2+} and suggests more thermodynamic susceptibility to corrosion. These electrochemical studies suggest strong modification of electrochemical behavior of the electrode using only an electrolyte additive to protect the PbAg anode from corrosion; Co, in this case, is proposed to form a protective oxide layer on the anode to resist corrosion [13].

3.3. Ex-Situ Coating

While the prior two water oxidation catalysts applied to the system are oxides formed in-situ and rapidly dissolved under the highly acidic conditions of zinc electrolysis, there are certain advantages to adopting a pre-applied heterogeneous catalyst with higher activity. First, it reduces complexity of the electrolyte solution and waste manganese. Second, reduction in manganese consumption is a cost driver for zinc refining, as is reduction in electricity consumption, both of which could be tackled by a competent heterogeneous water oxidation catalyst. This strategy is also proven, as iridium is used in the electrochemical industry as an anode protective layer, but is costly [28,29]. In this study, we investigate the properties of a pre-applied cobalt oxide-based catalyst, Co-dppe, to investigate how the surface electrochemistry of the Pb anodes is changed compared to the Co- and Mn-based solution phase additives that form catalytic layers in-situ.

Co-dppe was drop-coated onto the PbAg anodes using the same methods that had been used successfully on stainless steel alkaline electrolyzers [12]. Approximately 10 mg was enough to fully coat the anode; a truly active and stable heterogeneous catalyst should utilize substantially less Co than is required for in-situ production of a Co oxide protective layer from Co^{2+} [30–32]. While prior to electrolysis, the Co-dppe-coated electrode E_{corr} was 14 mV more positive than an equivalent electrode without the Co-dppe, both the E_{corr} measured during dynamic polarization and the surface potential under resting conditions both after reduction and if oxidized and left overnight, are more negative than the bare electrode, as seen below in Table 3.

Table 3. E_{corr} values (V vs. RHE) measured under open-circuit conditions during different equilibrium states of the PbAg electrode in 1.6 M H_2SO_4 . The “Polarized Equilibrium” state accessed by LSV after electrolysis is highlighted in bold below.

Solution Additive	Pre-Electrolysis E_{corr} (V)	Highly Polarized E_{corr} (V)	Polarized Eq. E_{corr} (V)	Resting Eq. E_{corr} (V)
None	−0.26	1.69	0.14	0.01
Co-dppe	−0.11	1.69	0.01	−0.06

In stark contrast to the in-situ coatings, an ex-situ applied water oxidation catalyst reduces the E_{corr} , suggesting that the electrode is thermodynamically more susceptible to corrosion. CA at an applied potential of 2.06 V vs. RHE over 30 min gave minimal current, as shown in Figure 5. An OCP measurement after polarization, however, gave the same highly polarized surface as in all other tests at 1.69 V vs. RHE. CP at an applied current density of $50 \text{ mA}\cdot\text{cm}^{-2}$ over 30 min gave an increase in the water oxidation overpotential compared to the PbAg electrode (2.39 V vs. RHE).

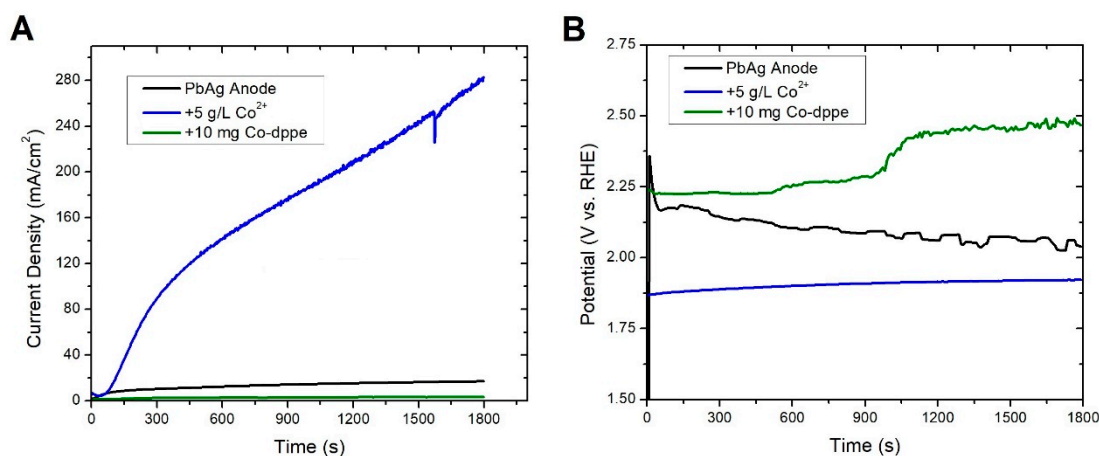


Figure 5. (A) Chronoamperograms at constant potential (2.06 V vs. RHE) and (B) chronopotentiograms comparing the Co²⁺-containing electrolyte (in blue), PbAg anode without any water oxidation catalytic metal additives (black), and Co-dppe coated PbAg anode (green).

These electrochemical studies and visual observation made it evident that the water oxidation catalyst flaked off of the electrode during the experiment. The mechanical and chemical instability of the water oxidation catalyst on the electrode surface exacerbated anode corrosion, thus when designing catalytic materials for anticorrosion applications, it is crucial for the chemical and mechanical stability of the catalyst to match the working environment. In this case, the Co-dppe initially appears to act as an anticorrosion layer from the pre-electrolysis OCP measurements, but after electrolysis acts as a cathodic reactant and may potentially accelerate corrosion of the underlying Pb.

4. Discussion

Anode corrosion and overpotential in the electrorefining and electrodeposition industries is a problem impacting the sustainability of metal production and plating. Metal products are typically produced at the cathode; for example, zinc in the case of electrowinning. The anode material that provides charge balance must remain intact for effective metal product formation to continue to occur at the cathode.

The harsh oxygen evolution reaction makes corrosion of anodes a challenge even for the most stable materials. In order to improve our understanding of how to protect anodes it is vital to understand how the current state-of-the-art systems operate. While prior studies have investigated corrosion rate, capacitance, and impedance of PbAg anodes with catalytic additives, there is still a significant gap in understanding how these additives affect oxygen evolution on PbAg anodes that are used in large-scale facilities, and further work must be done to determine molecular mechanisms.

One challenge in this field is measuring the thermodynamic properties of anodes, since it is well documented that the surface properties of PbAg anodes change rapidly as potentials are cycled [7,13]. With the recent advances toward understanding the role of Ag in PbAg anodes [8], we devised a method using high potential electrolysis followed immediately by voltammetry that allows us to measure OCPs of functioning systems. This method is sensitive to detect the improvement a catalyst makes to the system's oxygen evolution rate, as evidenced by the Co²⁺ and Mn²⁺ experiments. We also found that there are key restrictions under which conditions a heterogeneous catalyst can form a functional mixed oxide catalytic layer with a PbAg anode, requiring high-potential components to ensure that the catalyst material does not act as a cathodic reactant exacerbating corrosion.

Using the methods we outlined in this study, information on the surface potential of PbAg anodes under dynamic polarization conditions can be explored. This is a step toward understanding how catalytic additives interact with the anode surface to prevent anode corrosion. Going forward, we are

pursuing in-situ X-ray and electron microscopic analytical techniques to more accurately monitor surface potential, additive effects, and coordination of lead as dissolution occurs.

Supplementary Materials: The following are available online at <http://www.mdpi.com/2079-6412/8/7/246/s1>, Figure S1: Exemplary Linear Sweep Voltammograms, Table S1: Exchange Current Densities.

Author Contributions: S.W.S. designed the research and supervised the work; J.F.K.K. and S.W.S. planned the experiments and analyzed the data; J.F.K.K., C.C., and S.W.S. performed the experiments and wrote the manuscript.

Funding: This research was partially funded by a National Priorities Research Program grant (NPRP 10-0125-170246) from the Qatar National Research Fund (a member of The Qatar Foundation).

Acknowledgments: The authors acknowledge Chen-Lu Yang and the University of Massachusetts Center for Innovation and Entrepreneurship for facilities support.

Conflicts of Interest: The authors declare no conflict of interest.

References

1. Hunter, B.M.; Gray, H.B.; Muller, A.M. Earth-Abundant Heterogeneous Water Oxidation Catalysts. *Chem. Rev.* **2016**, *116*, 14120–14136. [[CrossRef](#)] [[PubMed](#)]
2. Clancy, M.; Bettles, C.J.; Stuart, A.; Birbilis, N. The influence of alloying elements on the electrochemistry of lead anodes for electrowinning of metals: A review. *Hydrometallurgy* **2013**, *131–132*, 144–157. [[CrossRef](#)]
3. Sheehan, S.W.; Cave, E.R.; Kuhl, K.P.; Flanders, N.; Smeigh, A.L.; Co, D.T. Commercializing Solar Fuels within Today's Markets. *Chem* **2017**, *3*, 3–7. [[CrossRef](#)]
4. Li, Y.; Gong, M.; Liang, Y.; Feng, J.; Kim, J.E.; Wang, H.; Hong, G.; Zhang, B.; Dai, H. Advanced zinc-air batteries based on high-performance hybrid electrocatalysts. *Nat. Commun.* **2013**, *4*, 1805. [[CrossRef](#)] [[PubMed](#)]
5. Winand, R. Electrodeposition of metals and alloys—New results and perspectives. *Electrochim. Acta* **1994**, *39*, 1091–1105. [[CrossRef](#)]
6. Tunnicliffe, M.; Mohammadi, F.; Alfantazi, A. Polarization Behavior of Lead-Silver Anodes in Zinc Electrowinning Electrolytes. *J. Electrochem. Soc.* **2012**, *159*, C170–C180. [[CrossRef](#)]
7. Zhang, W.; Houlachi, G. Electrochemical studies of the performance of different Pb–Ag anodes during and after zinc electrowinning. *Hydrometallurgy* **2010**, *104*, 129–135. [[CrossRef](#)]
8. McGinnity, J.J.; Nicol, M.J. The role of silver in enhancing the electrochemical activity of lead and lead-silver alloy anodes. *Hydrometallurgy* **2014**, *144–145*, 133–139. [[CrossRef](#)]
9. Mohammadi, M.; Alfantazi, A. The performance of Pb–MnO₂ and Pb–Ag anodes in 2 Mn(II)-containing sulphuric acid electrolyte solutions. *Hydrometallurgy* **2015**, *153*, 134–144. [[CrossRef](#)]
10. Cachet, C.; Le Pape-Rerolle, C.; Wiart, R. Influence of Co²⁺ and Mn²⁺ ions on the kinetics of lead anodes for zinc electrowinning. *J. Appl. Electrochem.* **1999**, *29*, 813–820. [[CrossRef](#)]
11. Bloomfield, A.J.; Sheehan, S.W.; Collom, S.L.; Crabtree, R.H.; Anastas, P.T. A heterogeneous water oxidation catalyst from dicobalt octacarbonyl and 1, 2-bis(diphenylphosphino) ethane. *New J. Chem.* **2014**, *38*, 1540–1545. [[CrossRef](#)]
12. Bloomfield, A.J.; Sheehan, S.W.; Collom, S.L.; Anastas, P.T. Performance Enhancement for Electrolytic Systems through the Application of a Cobalt-based Heterogeneous Water Oxidation Catalyst. *ACS Sustain. Chem. Eng.* **2015**, *3*, 1234–1240. [[CrossRef](#)]
13. Ivanov, I.; Stefanov, Y.; Noncheva, Z.; Petrova, M.; Dobrev, T.; Mirkova, L.; Vermeersch, R.; Demaerel, J.P. Insoluble anodes used in hydrometallurgy: Part I. Corrosion resistance of lead and lead alloy anodes. *Hydrometallurgy* **2000**, *57*, 109–124. [[CrossRef](#)]
14. Carr, J.P.; Hampson, N.A. The Lead Dioxide Electrode. *Chem. Rev.* **1972**, *72*, 679–703. [[CrossRef](#)]
15. Takehara, Z.-I. Dissolution and precipitation reactions of lead sulfate in positive and negative electrodes in lead acid battery. *J. Power Sources* **2000**, *85*, 29–37. [[CrossRef](#)]
16. Delahy, P.; Pourbaix, M.; Van Rysselberghe, P. Potential-pH Diagram of Lead and its Applications to the Study of Lead Corrosion and to the Lead Storage Battery. *J. Electrochem. Soc.* **1951**, *98*, 57–64. [[CrossRef](#)]
17. Koshel, N.D.; Gerasika, N.S.; Kostyrya, M.V. Nonstationary processes that occur on nonpolarizable lead surface in sulfuric acid. *Surf. Eng. Appl. Electrochem.* **2016**, *52*, 23–31. [[CrossRef](#)]

18. Vanysek, P. Electrochemical Series. In *Handbook of Chemistry and Physics*, 3rd ed.; Haynes, W.M., Ed.; CRC Press: Boca Riton, FL, USA, 2012.
19. Lai, Y.Q.; Li, Y.; Jiang, L.X.; Lv, X.J.; Li, J.; Liu, Y.X. Electrochemical performance of a Pb/Pb-MnO₂ composite anode in sulfuric acid solution containing Mn²⁺. *Hydrometallurgy* **2012**, *115–116*, 64–70. [[CrossRef](#)]
20. Newnham, R.H. Corrosion rates of lead based anodes for zinc electrowinning at high current densities. *J. Appl. Electrochem.* **1992**, *22*, 116–124. [[CrossRef](#)]
21. Nikoloski, A.N.; Nicol, M.J. Addition of Cobalt to Lead Anodes used for Oxygen Evolution—A Literature Review. *Miner. Process. Extr. Metall. Rev.* **2009**, *31*, 30–57. [[CrossRef](#)]
22. Zhang, W.; Ghali, E.; Houlachi, G. Performance of Pb-Ag anodes during polarisation and decay periods in zinc electrowinning. *Can. Metall. Q.* **2013**, *52*, 123–131. [[CrossRef](#)]
23. Li, Y.; Jiang, L.X.; Lv, X.J.; Lai, Y.Q.; Zhang, H.L.; Li, J.; Liu, Y.X. Oxygen evolution and corrosion behaviors of co-deposited Pb/Pb-MnO₂ composite anode for electrowinning of nonferrous metals. *Hydrometallurgy* **2011**, *109*, 252–257. [[CrossRef](#)]
24. Mondschein, J.S.; Callejas, J.F.; Read, C.G.; Chen, J.Y.C.; Holder, C.F.; Badding, C.K.; Schaak, R.E. Crystalline Cobalt Oxide Films for Sustained Electrocatalytic Oxygen Evolution under Strongly Acidic Conditions. *Chem. Mater.* **2017**, *29*, 950–957. [[CrossRef](#)]
25. Meruva, R.K.; Meyerhoff, M.E. Mixed Potential Response Mechanism of Cobalt Electrodes toward Inorganic Phosphate. *Anal. Chem.* **1996**, *68*, 2022–2026. [[CrossRef](#)] [[PubMed](#)]
26. Olesen, B.H.; Avci, R.; Lewandowski, Z. Manganese dioxide as a potential cathodic reactant in corrosion of stainless steels. *Corros. Sci.* **2000**, *42*, 211–227. [[CrossRef](#)]
27. Fukushima, S. Studies on Electrolytic Refining of Zinc. VII Effects of Manganese on Corrosion of Lead Anode. *Sci. Rep. Res. Inst. Tohoku Univ. Ser. A* **1960**, *12*, 456–468.
28. Kulandaisamy, S.; Rethinaraj, J.P.; Shockalingam, S.C.; Visvanathan, S.; Venkateswaran, K.V.; Ramachandran, P.; Nandakumar, V. Performance of catalytic activated anodes in the electrowinning of metals. *J. Appl. Electrochem.* **1997**, *27*, 579–583. [[CrossRef](#)]
29. Chen, C.; Bloomfield, A.J.; Sheehan, S.W. Selective Electrochemical Oxidation of Lactic Acid Using Iridium-Based Catalysts. *Ind. Eng. Chem. Res.* **2017**, *56*, 3560–3567. [[CrossRef](#)]
30. Goberna-Ferrón, S.; Soriano-López, J.; Galán-Mascarós, J.R. Activity and Stability of the Tetramanganese Polyanion [Mn₄(H₂O)₂(PW₉O₃₄)₂]¹⁰⁻ during Electrocatalytic Water Oxidation. *Inorganics* **2015**, *3*, 332–340. [[CrossRef](#)]
31. Li, J.; Güttinger, R.; Moré, R.; Song, F.; Wan, W.; Patzke, G.R. Frontiers of water oxidation: The quest for true catalysts. *Chem. Soc. Rev.* **2017**, *46*, 6124–6147. [[CrossRef](#)] [[PubMed](#)]
32. Jiao, F.; Frei, H. Nanostructured cobalt and manganese oxide clusters as efficient water oxidation catalysts. *Energy Environ. Sci.* **2010**, *3*, 1018–1027. [[CrossRef](#)]

